International Journal of Mechanical and Materials Engineering (IJMME), Vol. 5 (2010), No. 1, 80-86.

FINITE DIFFERENT AND LATTICE BOLTZMANN MODELLING FOR SIMULATION OF NATURAL CONVECTION IN A SQUARE CAVITY

C.S.N. Azwadi[1] and M.S. Idris[2]
[1]Faculty of Mechanical Engineering, Universiti Teknologi Malaysia, Skudai, Johor, Malaysia,
[2]Faculty of Mechanical Engineering, Universiti Malaysia Pahang, Kuantan, Pahang, Malaysia,
Email: azwadi@fkm.utm.my

ABSTRACT

In this paper, we report the characteristic of heat transfer and fluid flow behavior in a cavity with differentially heated side walls. Dirichlet type of boundary conditions was considered for the bottom and top walls, which is perfectly conducting boundary conditions. Three numerical experiments were preformed in order to study these phenomena at different Rayleigh numbers. In current study, the governing Navier-Stokes equations were solved directly by using finite different formulation and indirectly by using lattice Boltzmann method. The results for this problem were compared well between these two approaches. Good agreement also found when the computed results were compared with those published in literature.

Keywords: Finite Different Method, Lattice Boltzmann Method, Stream Function-Vorticity, Double Population, Natural Convection

NOMENCLATURE

c_p	Specific Heat
k	Heat conduction coefficient
g	Gravitational acceleration
T_H	Hot wall temperature
T_C	Cold wall temperature
u	Horizontal fluid flow velocity
v	Vertical fluid flow velocity

1. INTRODUCTION

The natural or free convection is the phenomenon of heat transfer between a surface and a fluid moving over it with the fluid motion caused entirely by the buoyancy forces that arise due to the density changes that result from the temperature variations in the flow. Since the early works by researchers (Lee et al., 1969, Clifton et al 1969, Hassan et al.,1970, Hasanuzzaman et al, 2007) a great deal of theoretical and experimental researches was dedicated to investigate this phenomenon. The fundamental interest comes from the concern to understand the heat transfer mechanism (Qi et al., 2008, Azwadi et al., 2006, Laguerre et al., 2005) and fluid flow behavior around the surfaces (Ravnik et al., 2008, Yasin et al., 2009). On the other hand, a similar interest was provoked by the wide range of engineering applications utilizing this type of phenomenon (Kobus, 2005, Laguerre et al., 2009). Among the problems related to natural convection, many researchers focused their investigation on the heat transfer and fluid flow behavior from a differentially heated side walls in a cavity (Azwadi et al., 2007, Lo et al., 2007, Hasanuzzaman et al, 2009). They frequently considered adiabatic boundary condition for the top and bottom walls. However, very few investigated the effect of perfectly conducting top and bottom walls although it plays important roles in real engineering applications (Patrick et al., 1999). In present study, we carried out numerical investigation of natural convection in a square cavity by considering perfectly conducting boundary condition for top and bottom walls. The left and right walls were maintained at hot and cold temperature respectively. The aspect ratio is restricted to unity. The objective of this paper is to gain better understanding of heat transfer mechanism and fluid flow behavior for the case in hand. In order to do this, we carried out numerical investigation based on two approaches; the lattice Boltzmann and finite different methods.

This paper is arranged as follow. The physics and the boundary conditions of the problem are firstly defined, followed by an explanation of the mathematical and numerical methods. Then, the results are presented and discussed. The last section concludes current study.

2. PROBLEM PHYSICS AND BOUNDARY CONDITIONS

The physical domain of the problem is represented in Fig. 1. The temperature difference between the left

and right walls introduces a temperature gradient in a fluid, and a consequent density difference induces a fluid motion, that is, convection. The top and bottom walls are considered made from a material that has a relatively high thermal conductivity. Therefore, it is usual to assume that the temperature on these walls varies linearly with distance from hot left to cold right walls.The Boussinesq approximation is applied to the buoyancy force term. With this approximation, it is assumed that all fluid properties can be considered as constant in the body force term except for the temperature dependence of the density in the gravity term.

$$\mathbf{G} = \beta g_0 (T - T_m)\mathbf{j} \tag{1}$$

where β is the thermal expansion coefficient, g_0 is the acceleration due to gravity, T_m is the average temperature and $\mathbf{j}$ is the vertical direction opposite to that of gravity.

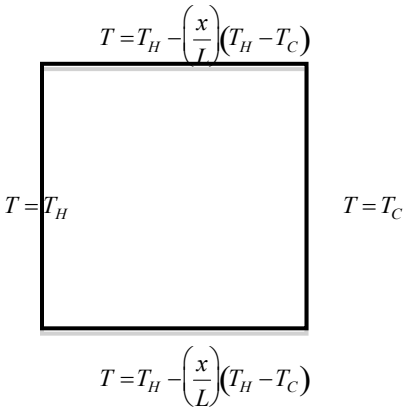

Figure 1. Physical domain of the problem.

The dynamical similarity depends on two dimensionless parameters: the Prandtl number *Pr* and Rayleigh number *Ra*,

$$Pr = \frac{\upsilon}{\chi} \tag{2}$$

$$Ra = \frac{\rho\beta(T_H - T_C)L^3}{\upsilon\chi} \tag{3}$$

where υ, χ and L are the fluid kinematic viscosity, thermal diffusivity and width of the cavity respectively.

In all simulations, *Pr* is set to be 0.71 and through the grid dependence study, the grid sizes of 101 × 101 for $Ra = 10^3$, 151 × 151 for $Ra = 10^4$ and 201 × 201 for $Ra = 10^5$ are found to be sufficient.

3. NUMERICAL MODELS

In this study, the governing equation of incompressible, two-dimensional and laminar Navier-Stokes and energy equations were solved directly using stream function-vorticity finite difference formulation and indirectly using lattice Boltzmann approach.

3.1 Stream function-vorticity finite differet approach

The conservation equations for this problem can be written as:

$$\frac{\partial u}{\partial x} + \frac{\partial v}{\partial y} = 0 \tag{4}$$

$$u\frac{\partial u}{\partial x} + v\frac{\partial u}{\partial y} = -\frac{1}{\rho}\frac{\partial p}{\partial x} + \upsilon\left(\frac{\partial^2 u}{\partial x^2} + \frac{\partial^2 u}{\partial y^2}\right) \tag{5}$$

$$u\frac{\partial v}{\partial x} + v\frac{\partial v}{\partial y} = -\frac{1}{\rho}\frac{\partial p}{\partial y} + \upsilon\left(\frac{\partial^2 v}{\partial x^2} + \frac{\partial^2 v}{\partial y^2}\right) + \beta g(T - T_1) \tag{6}$$

$$u\frac{\partial T}{\partial x} + v\frac{\partial T}{\partial y} = \left(\frac{k}{\rho c_p}\right)\left(\frac{\partial^2 T}{\partial x^2} + \frac{\partial^2 T}{\partial y^2}\right) \tag{7}$$

The pressure terms are eliminated by taking the *y*-derivative of (6) and subtracting from it the *x*-derivative of (5). This gives

$$u\left(\frac{\partial^2 v}{\partial x^2} - \frac{\partial^2 u}{\partial x \partial y}\right) + v\left(\frac{\partial^2 v}{\partial y \partial x} - \frac{\partial^2 u}{\partial y^2}\right) + \frac{\partial v}{\partial x}\left(\frac{\partial u}{\partial x} + \frac{\partial v}{\partial y}\right) - \frac{\partial u}{\partial y}\left(\frac{\partial u}{\partial x} + \frac{\partial v}{\partial y}\right) = \upsilon\left[\left(\frac{\partial^3 v}{\partial x^3} - \frac{\partial^3 u}{\partial x^2 \partial y}\right) + \left(\frac{\partial^3 v}{\partial y^2 \partial x} - \frac{\partial^3 u}{\partial y^3}\right)\right] - \beta g\frac{\partial T}{\partial x} \tag{8}$$

Using the definition of vorticity and continuity equation, (8) can be written as:

$$u\frac{\partial \omega}{\partial x} + v\frac{\partial \omega}{\partial y} = \upsilon\left(\frac{\partial^2 \omega}{\partial x^2} + \frac{\partial^2 \omega}{\partial y^2}\right) - \beta g\frac{\partial T}{\partial x} \tag{9}$$

In terms of the stream function, this equation becomes

$$\frac{\partial \psi}{\partial y}\frac{\partial \omega}{\partial x}-\frac{\partial \psi}{\partial x}\frac{\partial \omega}{\partial y}=\upsilon\left(\frac{\partial^2 \omega}{\partial x^2}+\frac{\partial^2 \omega}{\partial y^2}\right)-\beta g\frac{\partial T}{\partial x} \qquad (10)$$

In terms of the stream function, the equation defining the vorticity becomes

$$\left(\frac{\partial^2 \psi}{\partial x^2}+\frac{\partial^2 \psi}{\partial y^2}\right)=-\omega \qquad (11)$$

while in terms of the stream function, the energy equation becomes

$$\frac{\partial \psi}{\partial y}\frac{\partial T}{\partial x}-\frac{\partial \psi}{\partial x}\frac{\partial T}{\partial y}=\left(\frac{k}{\rho c_p}\right)\left(\frac{\partial^2 T}{\partial x^2}+\frac{\partial^2 T}{\partial y^2}\right) \qquad (12)$$

Before considering the numerical solution to the above set of equations, it is convenient to rewrite the equations in terms of dimensionless variables. The following dimensionless variables will be used here:

$$\Psi=\frac{\psi Pr}{\upsilon},\ \Omega=\frac{\omega L^2 Pr}{\upsilon}$$
$$X=\frac{x}{L},\ Y=\frac{y}{L} \qquad (13)$$
$$\theta=\frac{T-T_C}{T_H-T_C}$$

In terms of these variables, (9), (10) and (11) becomes

$$\frac{\partial^2 \Omega}{\partial X^2}+\frac{\partial^2 \Omega}{\partial Y^2}=\frac{1}{Pr}\left(\frac{\partial \Psi}{\partial Y}\frac{\partial \Omega}{\partial X}-\frac{\partial \Psi}{\partial X}\frac{\partial \Omega}{\partial Y}\right)+Ra\frac{\partial \theta}{\partial X} \qquad (14)$$

$$\frac{\partial^2 \Psi}{\partial X^2}+\frac{\partial^2 \Psi}{\partial Y^2}=-\Omega \qquad (15)$$

$$\frac{\partial^2 \theta}{\partial X^2}+\frac{\partial^2 \theta}{\partial Y^2}=\frac{\partial \Psi}{\partial Y}\frac{\partial \theta}{\partial X}-\frac{\partial \Psi}{\partial X}\frac{\partial \theta}{\partial Y} \qquad (16)$$

Finally, (14), (15) and (16) are solved using an iterative, uniform mesh finite different solution procedure with second order spatial accuracy.

3.2 Lattice Boltzmann Approach

As an alternative approach, the thermal fluid flow governing equations are solved indirectly using lattice Boltzmann method (LBM). Unlike other numerical methods, LBM predicts the evolution of particle distribution function and calculates the macroscopic variables by taking moment to the distribution function. LBM starts with the Boltzmann equation, discretised in space and time, given as:

$$f_i\left(\mathbf{x}+\mathbf{c}_i\Delta t, t+\Delta t\right)-f_i\left(\mathbf{x}, t\right)=-\frac{1}{\tau_f}\left(f_i-f_i^{eq}\right)+F \qquad (17)$$

$$g_i\left(\mathbf{x}+\mathbf{c}_i\Delta t, t+\Delta t\right)-g_i\left(\mathbf{x}, t\right)=-\frac{1}{\tau_g}\left(g_i-g_i^{eq}\right) \qquad (18)$$

where distribution function f is used to calculate density and velocity fields and distribution function g is used to calculate temperature field. F is the external force and τ_f and τ_g are the relaxation times carried by the momentum and energy respectively.

The equilibrium distribution functions f_i^{eq} and g_i^{eq} are chosen so that they satisfy the macroscopic equations ((4), (5), (6) and (7)) via Chapman-Enskog expansion. They can be written as (Azwadi et al., 2008):

$$f_i^{eq}=w_i\rho\left[1+3\mathbf{c}_i\cdot\mathbf{u}+4.5\left(\mathbf{c}_i\cdot\mathbf{u}\right)^2-1.5\mathbf{u}^2\right] \qquad (19)$$

$$g_i^{eq}=w_i\rho T\left[1+3\mathbf{c}_i\cdot\mathbf{u}+4.5\left(\mathbf{c}_i\cdot\mathbf{u}\right)^2-1.5\mathbf{u}^2\right] \qquad (20)$$

The values of the weight w_i depend on the chosen lattice model. In present study, we chose nine-velocity lattice model to represent both the f and g distribution functions. The lattice configuration is shown in Fig. 2.

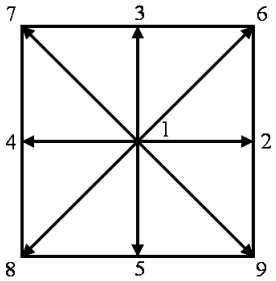

Figure 2. Nine-velocity lattice model with w_1 = 4/9, $w_{2,3,4,5}$ = 1/9 and $w_{6,7,8,9}$ = 1/36.

The macroscopic variables such as density, velocity and temperature can be calculated by taking moment to the distribution functions as follow:

$$\rho = \sum_{1}^{9} f_i,\ \rho \mathbf{u} = \sum_{1}^{9} \mathbf{c}_i f_i,\ \rho T = \sum_{1}^{9} \mathbf{c}_i g_i \quad (21)$$

The time relaxations can be related to the macroscopic fluid kinematic viscosity and thermal diffusivity using the following equations:

$$\tau_f = 3\upsilon + \frac{1}{2} \quad (22)$$

$$\tau_g = 3\chi + \frac{1}{2} \quad (23).$$

Via the so-called Chapmann-Enskog expansion, the evolution equations of distribution function could recover the macroscopic governing equations up to second order accuracy in space and time.

4. RESULTS AND DISCUSSION

In the previous section, we have discussed two numerical approaches to predict the phenomenon of natural convection in a square cavity. In this section, we shall apply the methods and demonstrate the obtained results in terms of the Nusselt number when the top and bottom walls are firstly set at adiabatic boundary condition. The benchmark results for two dimensional (Davis, 1983) and three dimensional (Tric et al., 2000) cases are brought for the sake of code validation. Then the comparison of the two approaches will be made in terms of isotherms plots and computed average Nusselt number in the system with the perfectly conducting boundary conditions applied at the top and bottom walls. Finally, the streamlines and contour of velocity components are plotted to demonstrate the effect of Rayleigh number on the fluid flow behavior.

Table 1. Comparison of average Nusselt number for natural convection heat transfer phenomenon

	$Ra = 10^3$	$Ra = 10^4$	$Ra = 10^5$
FD Approach	1.118	2.224	4.420
LBM	1.117	2.236	4.549
2-D solution	1.116	2.234	4.510
3-D solution	1.087	2.100	4.361

Table 1 shows the comparisons among the LBM and finite different approaches described in the previous sections, and two-and three-dimensional (2D and 3D) solutions to the Navier-Sokes equations. As can be seen from the table, the results predicted by the finite different and lattice Boltzmann methods generally compare well with the previous studies. There are some small differences between the results using finite different method for high Rayleigh number. However, these discrepancies are within three percents and can be accepted in real engineering applications.

From Table 1, we can see that for $Ra = 10^3$, the average Nusselt number is around 1.117, while for the 3D cubic cavity, the average Nusselt number is 1.087. The 3D result of the average Nusselt number is smaller than that in the two dimensional case, which shows the effect of the side walls. The same trend is applied to $Ra = 10^4$ and $Ra = 10^5$.

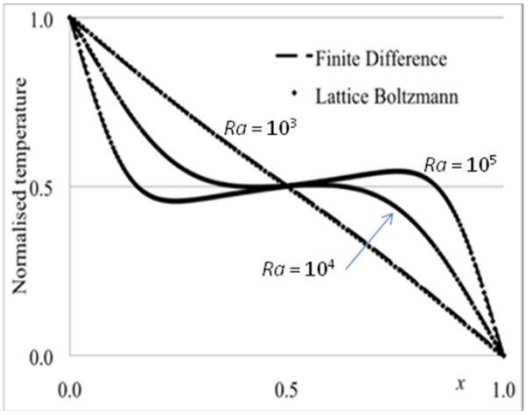

Figure 3. Normalised temperature profile at mid-height of the cavity.

Fig. 3 shows the normalized temperature profile given at the mid-height of the cavity for the laminar flow simulations with perfectly conducting boundary condition. The profiles show the rapid change in the heat transfer mechanism from conduction to convection. From a 45^0 slope at low Rayleigh number, the temperature profiles become horizontal lines in the cavity center and all temperature gradients are located in the interior of the boundary layer, which has developed near the vertical walls. Near the center of the cavity, the curves change slope and there is a vortex corresponding to its changes. It can be clearly seen that the steep variation of the temperature near the walls is resolved quite well.

Table 2 shows the average Nusselt number computed by finite different and lattice Boltzmann methods. Good agreement can be seen for the whole range of Rayleigh numbers. Compared to the results tabulated in Table 1, smaller value of computed average Nusselt number can be seen due to the heat release through the top and bottom walls for this case.

Table 2. Comparison of average Nusselt between finite different and lattice Boltzmann methods

	$Ra = 10^3$	$Ra = 10^4$	$Ra = 10^5$
FD Approach	1.046	1.766	3.489
LBM	1.056	1.907	3.517

The comparison of results obtained from the lattice Boltzmann and finite difference formulation is demonstrated in Fig. 4, which represents the plots of isotherms for every Rayleigh number.

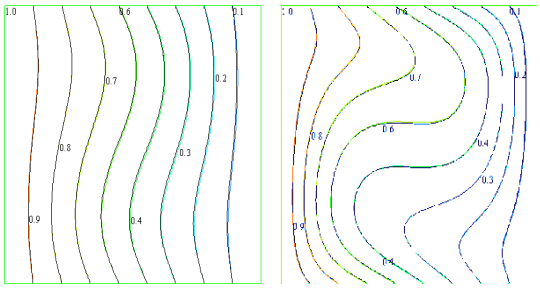

(a) $Ra = 10^3$ (b) $Ra = 10^4$

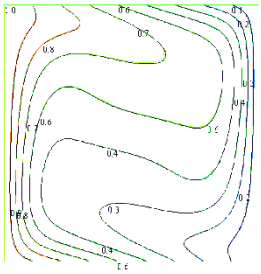

(c) $Ra = 10^5$

Figure 4. Isotherms plot for every Rayleigh numbers; coloured lines (finite difference), black lines (lattice Boltzmann).

As can be seen from Fig. 4, results from the lattice Boltzmann and finite different algorithms are in very good agreement for a wide range of Rayleigh number.

At $Ra = 10^3$, the isotherms are parallel to the heated walls, indicating that most of the heat transfer is by heat conduction. As the Rayleigh number increases ($Ra = 10^4$), the effect of convection can be seen in the isotherms where they become horizontal line at the center of the cavity. At $Ra = 10^5$, thin temperature boundary layer can be seen near both sides of the vertical walls. The system mostly occupied by horizontal isotherms indicating that the convection dominates the mode heat transfer mechanism.

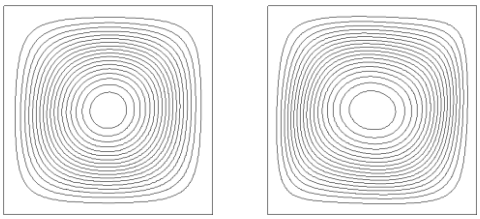

(a) $Ra = 10^3$ (b) $Ra = 10^4$

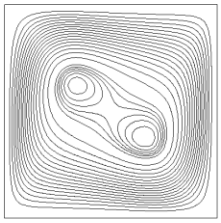

(c) $Ra = 10^5$

Figure 5. Streamline plots for various Rayleigh numbers.

Fig. 5 shows the streamlines plot for various values of Rayleigh number obtained from lattice Boltzmann method. Similar patterns are observed for those from the stream function-vorticity finite different formulation (not shown). They show that the hot fluid rises near to the hot left wall until it reaches the top wall, then moves along the horizontal wall before moving downwards along the right wall under the effect of cooling.

At $Ra = 10^3$, streamlines are those of a single vortex with its center in the center of the system. As the Rayleigh number increases ($Ra = 10^4$), the central streamline is distorted into an elliptic shape due to higher flow velocity along the top and bottom walls. At $Ra = 10^5$, the central streamline is elongated and two secondary vortices appear inside it. These vortices pointing towards the corners due to high magnitude of flow velocity drags the outer vortex along the vertical walls of the enclosure.

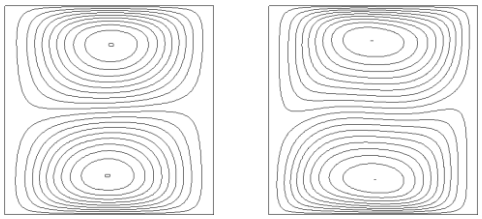

(a) $Ra = 10^3$ (b) $Ra = 10^4$

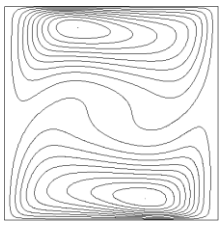

(c) $Ra = 10^5$

Figure 6. Contour plots for horizontal velocity components.

Contour plots for horizontal and vertical velocity components are shown in Fig. 6 and Fig. 7 respectively. From these figures, we can see that, as we increase the Rayleigh number, the isoline getting denser and denser near the walls. This indicates that the velocity maximum moves closer to the wall and its amplitude increases.

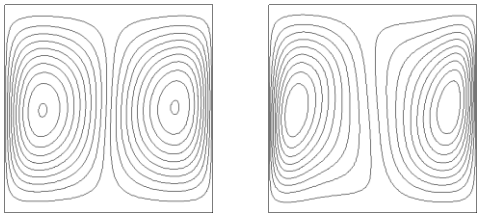

(a) $Ra = 10^3$ (b) $Ra = 10^4$

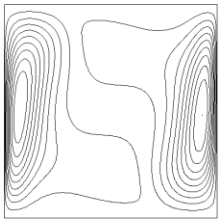

(c) $Ra = 10^5$

Figure 7. Contour plots for vertical velocity components.

5. CONCLUSSION

The natural convection in a differentially heated square cavity has been studied using finite different and lattice Boltzmann approaches. In finite different formulation, the Navier-Stokes equations were transformed into stream function-vorticity representation to reduce the number of unknown variables and hence reduce the computational time. In lattice Boltzmann formulation, the governing equation is solved using Lagrangian approach for the evolution of particles distribution function. Even though lattice Boltzmann approach required more computational time, however, due to the mesoscopic nature of the numerical analysis, this method contribute excellent numerical accuracy compared to other conventional numerical methods.

From Fig. 3 to Fig. 7, the boundary layers for the velocities and temperature can be observed clearly. As expected, the thermal boundary layer getting thinner and thinner as the Rayleigh number increases. The flow pattern including the boundary layers and vortices can be clearly seen. The heat transfer mechanism is also significantly influenced by the value of Rayleigh number. The results obtained demonstrate that the stream function-vorticity finite different and lattice Boltzmann formulations are reliable approaches to study flow and heat transfer in a differentially heated square enclosure.

ACKNOWLEDGMENT

Authors would like to thanks Universiti Teknologi Malaysia and Malaysia government for supporting this research activity.

REFERENCES

Clifton, J.V., Chapman, A.J., 1969. Natural Convection on a Finite-Size Horizontal Plate, International Journal of Heat and Mass Transfer 12, 1573–1584.

Hasanuzzaman, M., Saidur, R., Ali, M., Masjuki, H.H., 2007. Effects of Variables on Natural Convectve Heat Transfer trough V-Corrugated Vertical Plates, International Journal of Mechanical and Materials Engineering 2, 109–117.

Hasanuzzaman, M., Saidur, R and Masjuki, H.H., 2009. Effects of operating variables on heat transfer, energy losses and energy consumption of household refrigerator-freezer during the closed door operation, Energy 34(2), 196-198.

Hassan, K.E., Mohamed, S.A., 1970. Natural Convection from Isothermal Flat Surfaces, International Journal of Heat and Mass Transfer 13, 1873–1886.

Kobus, C.J., 2005. Utilizing Disk Thermistors to Indirectly Measure Convective Heat Transfer Coefficients for Forced, Natural and Combined (Mixed) Convection, Experiments in Thermal and Fluid Science 29, 659–669.

Laguerre, O., Amara, S.B., Flick, D., 2005. Experimental Study of Heat Transfer by Natural Convection in a Closed Cavity: Application in a Domestic Refrigerator, J. Food Engineering 70, 523–537.

Laguerre, O., Remy, D., Flick, D., 2009. Airflow, Heat and Moisture Transfers by Natural Convection in a Refrigerating Cavity, J. Food Engineering 91, 197–210.

Lee, S.L., Hellman, J.M., 1969. Study of Firebrand Trajectories in a Turbulent Swirling Natural Convection Plume, Combustion and Flame 13, 645-655.

Lo, D.C., Young, D.L., Tsai, C.C., 2007. High Resolution of 2D Natural Convection in a Cavity by the DQ Method, J. Computers and Applied Mathematics 203, 219–236.

Nor Azwadi, C.S., Tanahashi, T., 2006. Simplified Thermal Lattice Boltzmann in Incomressible Limit, International Journal of Modern Physics B 20, 2437-2449.

Nor Azwadi, C.S., Tanahashi, T., 2007. Three-Dimensional Thermal Lattice Boltzmann Simulation of Natural Convection in a Cubic Cavity, International Journal of Modern Physics B 21, 87–96.

Nor Azwadi, C.S., Tanahashi, T., 2008. Simplified Finite Difference Thermal Lattice Boltzmann Method, International Journal of Modern Physics B 22, 3865–3876.

Patrick, H.O., David, N., 1999. Introduction to Convective Heat Transfer Analysis. McGraw Hill.

Qi, H.D., 2008. Fluid Flow and Heat Transfer Characteristics of Natural Convection in a Square Cavities due to Discrete Source-Sink Pairs, Interntaional Journal of Heat and Mass Transfer 51, 25-26.

Ravnik, J., Skerget, L., Zunic, Z., 2008. Velocity-Vorticity Formulation for 3D Natural Convection in an Inclined Enclosure by BEM, International Journal Heat and Mass Transfer 51, 4517–4527.

Yasin, V., Hakan, F.O., Ahmet, K., Filiz, O., 2009. Natural Convection and Fluid Flow in Inclined Enclosure with a Corner Heater, Applied Thermal Engineering 29, 340–350.